Effects of temperature, mechanical state and their interactions on permeability of concrete

Marta Choinska, Abdelhafid Khelidj, Frédéric Dufour, Gilles Pijaudier-Cabot

EFFECTS OF TEMPERATURE, MECHANICAL STATE AND THEIR INTERACTIONS ON PERMEABILITY OF CONCRETE

EFFETS DE LA TEMPÉRATURE, DE L'ÉTAT MÉCANIQUE ET DE LEURS INTERACTIONS SUR LA PERMÉABILITÉ DU BÉTON DE STRUCTURE

Marta CHOINSKA[1], Abdelhafid KHELIDJ[2], Frédéric DUFOUR[1], Gilles PIJAUDIER-CABOT[1]
[1] *ERT R&DO, GeM / UMR CNRS 6183, Nantes, France*
[2] *ERT R&DO, GeM / UMR CNRS 6183, Saint Nazaire, France*

ABSTRACT - The objective of the presented study is to investigate the interactions between damage, temperature, stress level and permeability in structural concrete. The permeability tests are performed on hollow concrete cylinders, subjected to temperature up to 150 °C and compressive loading up to failure. The results emphasize that at stress levels lower than 80-85 % of the peak stress, the variation of permeability is small and it is slightly influenced by the stress. As the load exceeds 80-85 % of the peak stress and approaches the peak, damage increases rapidly causing an important increase of the permeability and a greater sensitivity to the applied load. Finally, the obtained results reveal that the effects of damage and temperature may be decoupled for the estimation of the concrete permeability.

***RÉSUMÉ* -** L'objectif de cette étude est de caractériser l'interaction entre endommagement, température, état de contrainte et perméabilité du béton de structure. Les mesures de la perméabilité sont effectuées sur des éprouvettes cylindriques soumises à des températures jusqu'à 150 °C et à une compression uniaxiale jusqu'à la rupture. Les résultats montrent que, pour un chargement inférieur à 80-85 % du chargement maximal, la variation de la perméabilité reste faible et peu influencée par le chargement. Quand le chargement excède 80-85 % du chargement maximal et approche le pic, l'endommagement croit rapidement, entraînant une augmentation importante de la perméabilité. Finalement, les résultats révèlent que les effets de l'endommagement et de la température peuvent être découplés pour l'estimation de l'évolution de la perméabilité.

1. Introduction

Transport properties of concrete, like permeability or diffusivity, influence the durability of the concrete structures by controlling the penetration rate of aggressive agents, but also directly if the structure has a confinement role, like confinement vessels of French nuclear power plants for instance. These structures, during their service life, are subjected to different types of loads (mechanical, thermal, chemical, restrained shrinkage, aging etc…). Generally service loads are not significant enough to cause an important degradation of structural concrete. However, with time, the degradation accumulates and may lead to micro-cracking resulting in permeability variations. This contribution aims directly at such confinement structures for which it is critical to evaluate their gas tightness and its evolution with time, both in the case where concrete remains in the pre-peak regime (typically in the normal service life) and also when it might reach locally the post-peak regime, e.g. during integrity tests or accidents, where an increase of temperature is also expected (up to 150 °C in the class of accidents considered in this paper).

Existence of the strong interaction between permeability and load-induced microcracking (diffused damage) has been proved by theoretical micro-macro justifications (Dormieux and Kondo, 2004 ; Chatzigeorgiou et al., 2005) and has been also observed experimentally. Studies on effect of uniaxial compressive stress on gas permeability have showed that permeability increases significantly when the load level reached 70-90 % of ultimate strength for concrete (Sugiyama et al., 1996 ; Hearn and Lok, 1998 ; Picandet et al., 2001). Some other studies (Wang et al., 1997) have emphasized a correlation between permeability and crack opening in the post-peak phase of the Brazilian splitting test.

Besides the applied load, another parameter which influences the permeability of concrete is temperature. Multiple phenomena at the microstructural level of the material take place during an elevation of temperature. Among the most important ones, there are a modification of the moisture content due to non-bounded water evaporation (up to 105 °C), chemical dehydration of cement paste due to loss of bounded water (beyond 105 °C), thermal expansion, porosity increase, thermal cracking due to thermal and mechanical incompatibility, etc. A considerable increase of permeability, if measured under temperature or after thermal treatment, has been observed experimentally (Tsimbrovska, 1998 ; Lion et al., 2005 ; Joos and Reinhardt, 2002). According to Gawin et al. (Gawin et al., 1999) a power relationship between temperature and concrete permeability should be considered.

Existing experimental data provide therefore some correlation between the mechanical state (micro-cracking and macro-cracking) and the permeability of concrete. The same exists for the influence of temperature on permeability of concrete but very little data is available on the coupled temperature and load effects on the permeability of concrete. In order to characterize the interaction between mechanical state, temperature and permeability of concrete, we propose to carry out an experimental study. For the sake of simplicity, the study is restricted to dry material. The tests are carried out on hollow concrete cylinders set up in a climatic chamber at controlled temperature (20 °C, 105 °C or 150 °C) and relative humidity (close to 0 %), and loaded in a uniaxial compression test up to failure. This test enables obtaining of two damage regimes: diffused one (homogenously diffused microcracks in the pre-peak phase) and localized one (localized macrocrack(s) in the post-peak phase).

In the current paper the developed experimental device and the testing procedure are first presented, while the results of the experimental study are shown and discussed in the following section. Finally, some concluding remarks are made in the last section.

2. Experimental program

2.1. Concrete composition and specimen curing

An ordinary concrete of water to cement ratio equal to 0.6 is used in this study. The hollow concrete cylinders (110x220 mm^2) have been cast in metal moulds. A cylindrical borehole has been cast in each specimen by placing a metallic bar (diameter of 14 mm) in the moulds.

All the specimens have been subjected to the same curing and conditioning processes. They were stored in water during 1 month and dried in a ventilated oven initially at 80 °C (during 1 month), then at 105 °C down to constant mass.

2.2. Measurements of gas permeability

A simplified diagram of the experimental device is shown in Figure 1 (a).

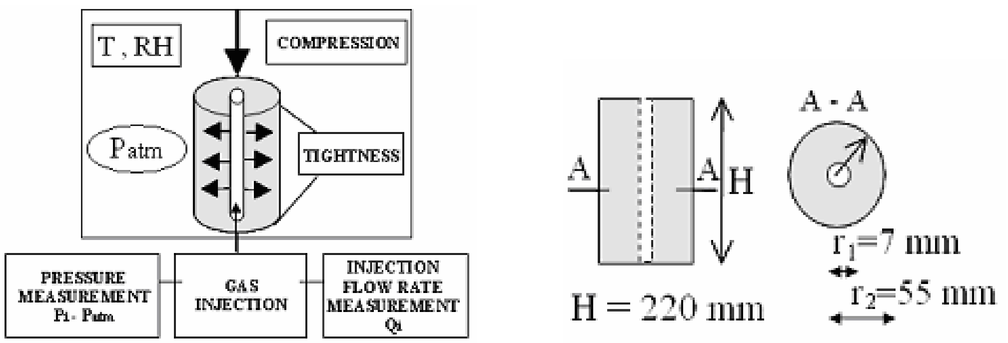

(a) (b)

Figure 1. (a) Simplified diagram of the experimental device. (b) Geometry of the specimen.

Permeability tests are performed for the steady state gas (nitrogen) radial flow in quasi-isothermal conditions. A relative pressure ΔP (difference between the injection pressure P_i and the atmospheric pressure P_{atm}) and mass flow rate are measured at the upstream of the specimen by the thermal Mass Flow Meter (MFM) which converts the mass flow rate to an equivalent volumetric gas flow rate.

Darcy's law and mass balance equation lead to the determination of an apparent permeability k_a [m^2]. When the injection flow rate Q_i [m^3/s] is known, the permeability k_a [m^2] may be calculated as follows:

$$k_a = \frac{Q_i \cdot P_i \cdot \mu \cdot \ln\left(\frac{r_2}{r_1}\right)}{\pi \cdot H \cdot \left(P_i^2 - P_{atm}{}^2\right)} \qquad (1)$$

where μ [Pa.s] is the dynamic viscosity of the inert gas used (nitrogen) and r_1 [m], r_2 [m], H [m] are the inner radius, outer radius, and the height of the cylindrical specimen respectively (see Figure 1 (b)).

This permeability is relative to the overall gas flow through the material, consisting of the viscous flow and the slip flow. In order to get an intrinsic permeability in the case of a laminar gas flow, a characteristic of the porous medium solely and being strictly relative to the viscous flow, Klinkenberg or Carman approach may be applied. In this study, the relationship due to Klinkenberg (Klinkenberg, 1941) is used:

$$k_a = k_v(1 + \frac{\beta}{P_m}) \tag{2}$$

where P_m [Pa] corresponds to the average gas pressure, $P_m = \frac{P_i + P_{atm}}{2}$ and β [Pa] is the Klinkenberg coefficient, a constant which is inversely proportional to the average diameter of the capillaries. The intrinsic permeability k_v [m^2] is obtained by extrapolating the apparent gas permeability k_a determined at various pressures to the case of an infinite pressure.

2.3. *Testing procedure*

In the pre-peak phase, the measurements of the apparent permeability are performed for five relative pressures: 0.30, 0.25, 0.20, 0.15, and 0.10 MPa. In the post-peak phase, the applied pressures are adapted to the measurable upstream flow rate. The latter is given by one of the three digital thermal Mass Flow Meters (MFM) of ranges: 10-500 ml/min, 20-1000 ml/min and 300-15000 ml/min respectively. A period of 2 to 5 minutes approximately is necessary in order to reach the steady state gas flow. During the test, the applied force, the stroke displacement, the displacements measured from the LVDTs, the injection and the atmospheric gas pressures and mass flow rate through the specimen are recorded. The accuracy of measurement of the apparent permeability is 2 % approximately. The full testing procedure is as follows:

- First, a measurement of the *initial permeability* of concrete is performed at 20 °C, with an axial compressive load of 4 kN, resulting in the compressive stress of 0.4MPa (negligible stress for this concrete). This load is needed for ensuring the tightness of the permeability cell (radial flow only). The initial permeability is subsequently used as a reference value in forthcoming comparisons.
- Then, the required temperature is applied (20 °C, 105 °C or 150 °C). During heating at a constant rate of 10 °C/h, the compressive load of 4 kN is kept. A stabilization period of temperature through the material is needed, thus permeability tests start after 60 hours, under a constant temperature. Prior to that, the *reference permeability* is measured again in order to obtain the effect of the temperature.
- Afterwards, the specimen is loaded with a displacement rate of 0.02 mm/min up to the required load level. Load levels correspond to 20, 40, 60, 80, 85 and 90 % of the estimated peak stress in the pre-peak regime, while close to the peak and in the post-peak phase each load level corresponds to an increase of axial strain of 0.3 mm/m. Each load level is maintained during 30 minutes in order to allow for the determination of the gas *permeability*. For each load level, once the permeability under load is measured, the specimen is unloaded down to 4 kN and the permeability of the unloaded specimen is measured.

All the results presented below refer to the values of intrinsic permeability obtained with four tests per temperature.

3. Results and discussion

The initial permeability of the concrete tested (prepared with three batches) varies between 6.10^{-17} m² and 12.10^{-17} m². This variation is relatively small and illustrates the good reproducibility of the material.

3.1. Evolution of permeability during loading and after unloading

The results emphasize that the ratio of loading to unloading permeability varies with the applied stress level and temperature. In the strain space (longitudinal strain measured with the LVDTs on the specimen), it may be represented by a function which reaches the values lower than one in the early pre-peak phase, reaches a maximum in early post-peak phase for a relative strain (maximum load induced strain to peak strain) equal to 1.1-1.2, and tends to become a constant further in the post-peak regime (the two permeabilities are equal). This relation is plotted in Figure 2 for the three tested temperatures.

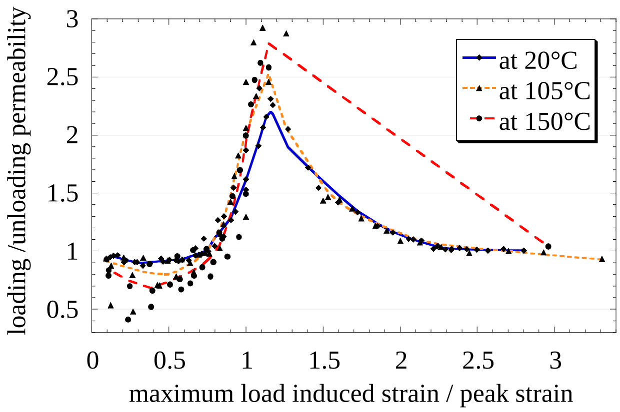

Figure 2. Loading to unloading intrinsic permeability ratio vs applied relative strain.

Low compressive stress levels act on the initial porosity by squeezing it (volume contraction), which yields a decrease of permeability. In this phase, unloading generates the opposite effect and thus the permeability increases (the behaviour is reversible).

Till relative strain equal to 0.7-0.8, which corresponds to 80-85 % of the peak stress, the permeability measured after unloading remains quasi-constant, while the permeability measured during loading slightly decreases and then increases, but is still lower than the initial permeability (Choinska et al., 2007). Possible micro-crack formation upon loading is compensated by the closure of existing pores. Upon unloading, cracks induced by the applied load may close while existing pores or cracks open again.

Beyond these stress levels, permeability measured during loading exceeds the values revealed after unloading. The amount of micro-crack formed is enough in order to compensate effect of closure of the initial microstructure. Consequently, the permeability measured during loading reaches greater values than after unloading.

3.2. Evolution of permeability in pre-peak and post-peak phases

The results presented in Figure 3 show the complete evolution of the relative permeability during loading and after unloading with the maximum applied relative strain for the three tested temperatures. It turns out that at the peak (relative strain equal to 1), the permeability becomes ten times its initial value approximately, if measured during loading at 105 °C and 150 °C, and up to five times its initial value, if measured at 20 °C. Up to the peak, the variation of the relative permeability is quite moderate in comparison to the post-peak phase.

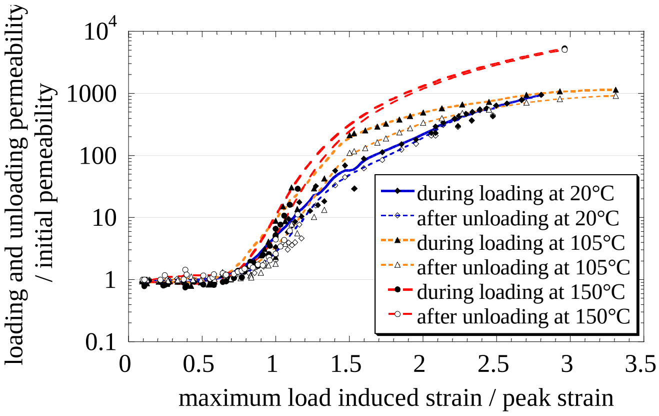

Figure 3. Variation of relative intrinsic permeability with maximum applied relative strain for the three tested temperatures.

Three regimes of variation of permeability, as a function of the strain of the specimen, are observed for all tested temperatures in Figure 3: the first one (up to a relative strain of 0.9), where the permeability varies relatively slightly, the second one (for a relative strain between 0.9 and 1.4), where the permeability increases rapidly and the third one, which is characterized by a steady and slower rate than the latter. These observations are in agreement with the experimental results obtained by Gérard (Gérard, 1996) and Wang et al. (Wang et al., 1997). The first regime corresponds probably to the fluid percolation through both the pores and diffused micro-cracks; the second one corresponds to the fluid flow through interconnected micro-cracks which initialise macro-cracks formation, while the third one is probably related to the localized fluid flow through the cracks only (Poiseuille flow).

3.3. Evolution of permeability with damage and temperature - Interaction law

Following the analysis by Picandet et al. (Picandet et al., 2001), it is more consistent in the pre-peak phase to record the evolution of the permeability with damage instead of the strain or stress. In order to analyze the effect of the applied load on permeability, we follow here the same procedure and compute damage from the variation of the unloading stiffness recorded on the mechanical response of the specimen. The result is shown in Figure 4 (a). On this plot, we have the permeability evaluated after unloading as a function of damage d defined as $d = \frac{E_0 - E_d}{E_0}$ where E_0 is the initial Young's modulus of the material and E_d is the unloading modulus. One may say that the evolution of the permeability due to the applied load for the three temperatures tested falls on the same master curve. Note that we have considered in this figure the permeability measured after unloading instead of the permeability measured under load, since it is expected that for the permeability measured under load, some load effect could be accounted for, or possibly neglected in the pre-peak phase (for conservative safety reasons, the decrease of permeability may be neglected).

The effect of the temperature on the permeability, measured with applied mechanical load, is shown in Figure 4 (b) for some damage levels. We observe that the evolution of the permeability with the temperature is almost the same for any state of damage considered.

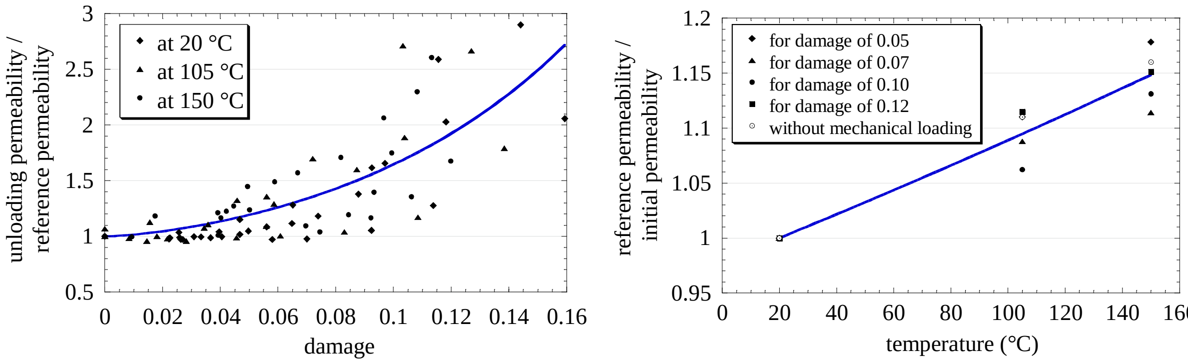

(a) (b)

Figure 4. (a) Variation of relative to mechanical state intrinsic unloading permeability with damage for the three tested temperatures (b) Variation of relative to temperature intrinsic permeability with temperature for different damage levels.

Therefore, one may possibly say that the overall evolution of the permeability follows a multiplicative format: *k=f(damage).g(temperature)*. The increase of permeability due to temperature and damage is the product of two functions (*f* and *g*) which reflect each contribution separately (Choinska et al., 2007). Our experimental results are also consistent with the formula proposed by Gawin and co-workers (Gawin et al., 1999).

4. Conclusions

The results reported in this study can be summarised as follows:

The effect of the applied stress is first a decrease of the permeability. This effect can be neglected in structural analyses; at least it should be conservative to do so for structural elements loaded in compression (such as confinement vessels). As micro-cracking develops, the reverse is observed and the permeability under load (beyond 80-85 % of the peak stress) becomes greater than upon unloading. Furthermore, micro-cracks do not close entirely upon stress reversal and the permeability during unloading increases. In the post-peak phase an important growth of permeability takes place due to the progressive crack opening and extension under compressive loading.

The increase of permeability with the applied load is greater with temperature, inducing further alterations and dilatation of concrete.

Finally, the experimental results in the pre-peak phase seem to agree with the format of coupled evolution of the permeability due to damage and temperature, assumed by Gawin et al. (Gawin et al., 1999). Obviously, this is not a general proof that the above relationship should hold for any concrete, temperature or damage, but experimental data are not in contradiction with it. Further studies with different concretes and a wider range of temperature are needed.

5. References

Chatzigeorgiou G., Picandet V., Khelidj A., Pijaudier-Cabot G. (2005) Coupling between progressive damage and permeability of concrete: analysis with a discrete model, *Int. J. Anal. Meth. Geomech.* **29**, 1005-1018.

Choinska M., Khelidj A., Chatzigeorgiou G., Pijaudier-Cabot G. (2007) Effects and Interactions of Temperature and Stress-level Related Damage on Permeability of Concrete, *Cement and Concrete Research* **37**, 79-88.

Dormieux L. and Kondo D. (2004) Approche micromécanique du couplage perméabilité-endommagement, *C.R. Mecanique* **332**, 135-140 (in french).

Gawin D., Majorana C. E., Schrefler B. A. (1999) Numerical analysis of hygro-thermal behaviour and damage of concrete at high temperature, *Mech. Cohes.-Frict. Mater.* **4**, 37-74.

Gérard B. (1996) Contribution des couplages mécanique-chimie-transfert dans la tenue à long terme des ouvrages de stockage de déchets radioactifs, Thèse de doctorat (PhD Thesis in French), ENS Cachan.

Hearn N. and Lok G., Measurement of Permeability under Uniaxial Compression-A Test Method, *ACI Materials Journal* **95** (1998) 691-694.

Joos M. and Reinhardt H.W. (2002) Permeability and diffusivity of concrete as function of temperature, *Cement and Concrete Research* **32**, 1497-1504.

Klinkenberg L.J. (1941) The permeability of porous media to liquids and gases, American Petroleum Institute, *Drilling and Production Practice*, 200-213.

Lion M., Skoczylas F., Lafhaj Z., Sersar M. (2005) Experimental study on a mortar. Temperature effects on porosity and permeability. Residual properties or direct measurements under temperature, *Cement and Concrete Research* **35**, 1937-1942.

Picandet V., Khelidj A., Bastian G. (2001) Effect of axial compressive damage on gas permeability of ordinary and high-performance concrete, *Cement and Concrete Research* **31**, 1525-1532.

Sugiyama T., Bremner T.W., Holm T.A. (1996) Effect of Stress on Gas Permeability in Concrete, *ACI Materials Journal* **93**, 443-450.

Tsimbrovska M. (1998) Dégradation des bétons à hautes performances soumis à des températures élevées. Evolution de la perméabilité en liaison avec la microstructure, Thèse de doctorat (PhD Thesis in French), Université Grenoble 1.

Wang K., Jansen D.C., Shah S.P., Karr A.F. (1997) Permeability study of cracked concrete, *Cement and Concrete Research* **27**, 381-393.